Electronic Supplementary Material (ESI) for Inorganic Chemistry Frontiers.

Supporting Information

Honeycomb carbon substrate anchored with Sn and Sb bimetallic atoms boosts oxygen reduction electrocatalysis

Shuting Li,[a] Jinxi Han,[a] Yuyu Guo,[a] Zhengqiang Xia,[a] Sanping Chen,[a]* Gang Xie,[a] Shengli Gao,[a] Qi Yang[a]*

[a] *Key Laboratory of Synthetic and Natural Functional Molecule of the Ministry of Education, College of Chemistry and Materials Science, Northwest University, Xi'an, Shaanxi, 710127, China.*

**Corresponding authors e-mail address: yangqi@nwu.edu.cn, sanpingchen@126.com*

Material characterization

The morphology details were observed by scanning electron microscopy (SEM, Apreo S) and transmission electron microscopy (TEM, Talos F200x, JEM-1400Flash) with energy dispersive X-ray spectrometer. The phase composition and structure of all samples were obtained on X-ray diffraction (XRD, D8 Advance). The chemical composition and valence were detected by X-ray photoelectron spectroscopyx (XPS, PHI-5000 Versa ProbeIII). The Raman spectra recorded on a Micro-Raman imaging spectrometer (Raman, DXR2). The specific surface area was tested and calculated using Brunauer-Emmett-Teller (BET, Tristar II 3020) method, samples were vacuum degassed at 150 ℃ for 6 hours.

Electrochemical measurements

The performance of the ORR was tested using a CS2350H electrochemical workstation. The classical three-electrode test method was used, with Ag/AgCl chloride as the reference electrode, the Pt electrode with a salt bridge as the counter electrode, and a rotary ring disk electrode with glass carbon (GC) as the working electrode. The SnSb-NC catalyst (5.0 mg) was dispersed in a solution of ethanol (400.0 μl), deionized water (90.0 μl) and Nafion 117 (10.0 μl), and the homogenized ink was obtained by ultrasonic detection for 30 minutes. Then, 12.0 μl of ink was dropped on the GC carefully and naturally air-dried as the working electrode. The electrolyte was placed in N_2/O_2 saturation before electrochemical testing. Cyclic voltammetry (CV) at a scan rate of 20 mV s^{-1} and linear scanning voltammetry (LSV) at different scan speeds (400 rpm-2500 rpm) were performed. All the test data obtained in this paper should be converted into a reversible hydrogen electrode (RHE) with the conversion formula $E_{RHE} = E_{Ag/AgCl} + 0.059\ pH + 0.197$.

Using disk current and ring current, the following equations were used to calculate hydrogen peroxide production (H_2O_2 %) and electron transfer number (n):

$$H_2O_2\,(\%) = \frac{200 * \frac{I_r}{N}}{I_d + \frac{I_r}{N}}$$

$$n = \frac{4 * I_d}{I_d + \frac{I_r}{N}}$$

Where I_r is the ring current, I_d is the disk current, and N is the ring-disk electrode with a collection coefficient of 0.47.

Assembly and test of zinc-air battery

Mix the catalyst (9.0 mg), PVDF (1.0 mg), and anhydrous sodium sulfate (1.0 mg) thoroughly. Subsequently, add 3 to 4 drops of 1-methyl-2-pyrrolidenone to the mixture and grind for 30 minutes until thickened. The catalyst slurry was evenly coated on the surface of the type P1 composite electrode after drying at 100 °C under static press pressure of 15 MPa for 30 minutes， as the cathode for the battery, the polished zinc sheet as the anode, and 6 M KOH + 0.2 M $Zn(Ac)_2{\cdot}2H_2O$ as the electrolyte. Open-circuit voltage (OCV) and power density were tested by the CS2350H Electrochemical Workstation. Specific capacity and constant current charge and discharge were passed by Blue Electric Test System test (5V1A8C).

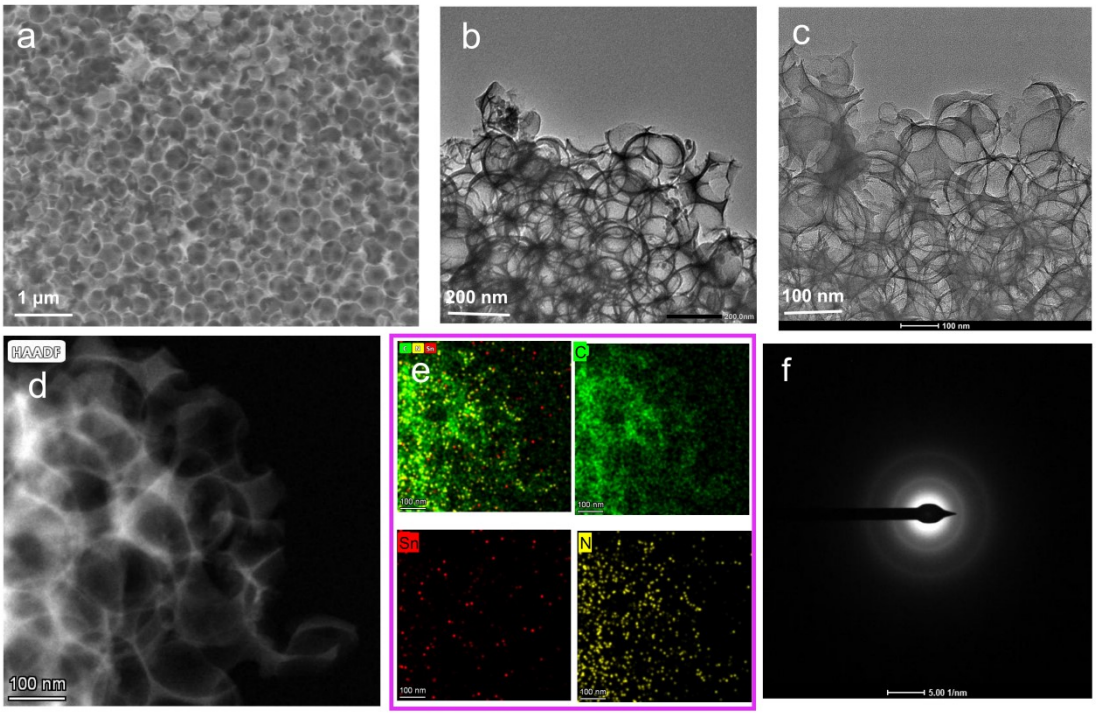

Figure S1. (a) SEM image of Sn-NC. (b-c) TEM images of Sn-NC. (d) HAADF-STEM image of Sn-NC. (e) Elemental mapping images of Sn-NC. (f) SAED pattern of Sn-NC.

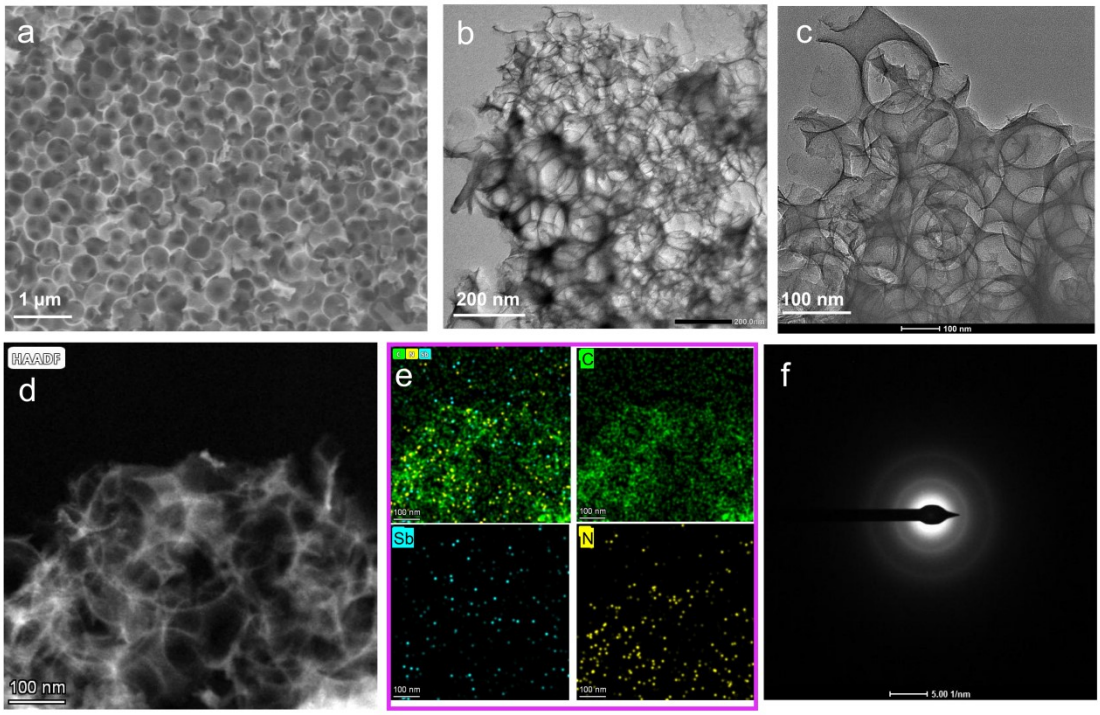

Figure S2. (a) SEM image of Sb-NC. (b-c) TEM images of Sb-NC. (d) HAADF-STEM image of Sb-NC. (e) Elemental mapping images of Sb-NC. (f) SAED pattern of Sb-NC.

The electron diffraction test of Sn-NC and Sb-NC showed that the carbon material had no stereotyped carbon.

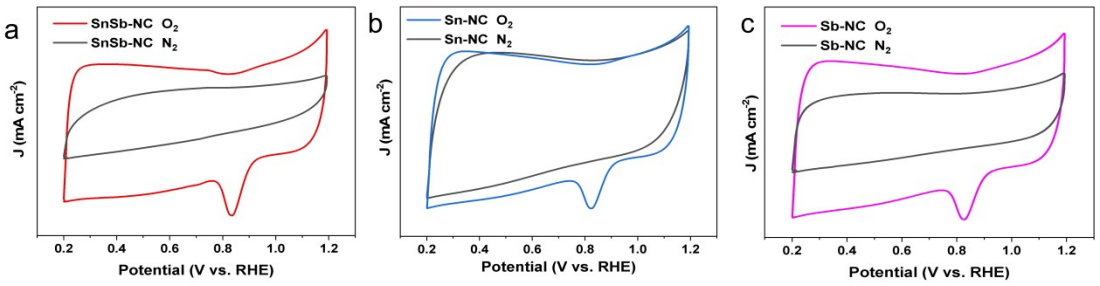

Figure S3. Cyclic voltammogram of the catalysts in 0.1 M KOH solution at O_2 and N_2 saturation.

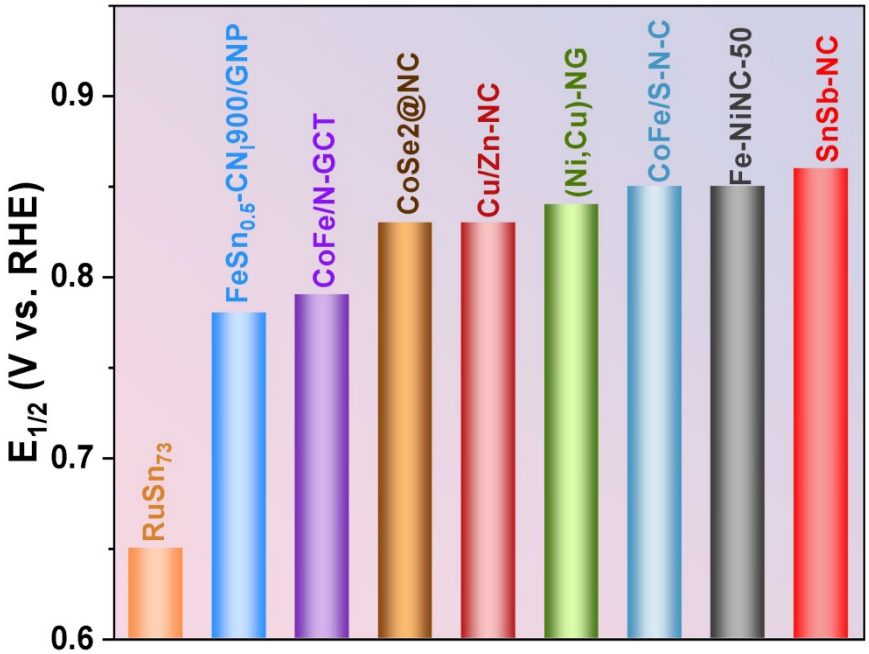

Figure S4. Comparison of the $E_{1/2}$ with recently reported catalysts. [1-8]

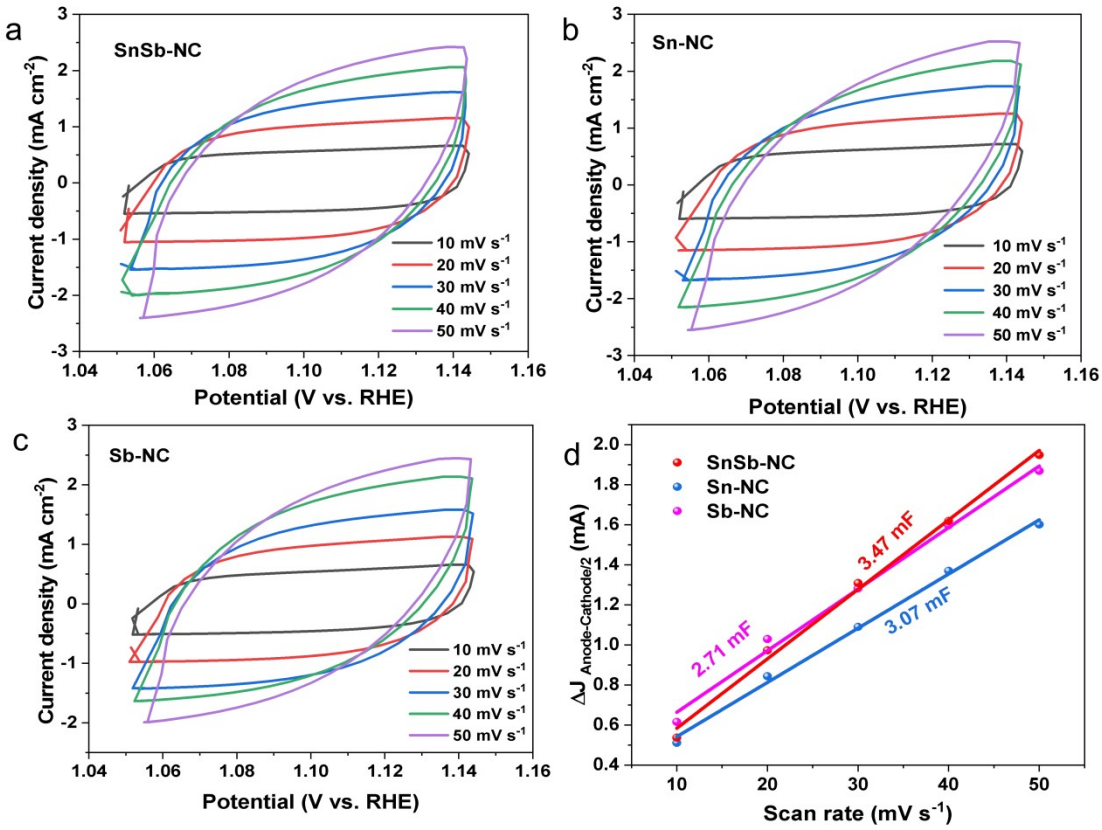

Figure S5. (a-c) electric double layer capacitance of catalysts. (d) CV fitting plots for different catalysts measured at non-Faradic regions.

Table S1. Atomic percentages of N were obtained by the deconvolutions of N 1s spectra.

Catalysts	N content (at. %)			
	Pyridinic N	Pyrrolic N	Graphite N	Oxidized N
SnSb-NC	15.81	7.82	60.22	16.15
Sn-NC	14.63	15.92	54.83	14.62
Sb-NC	13.14	8.37	53.14	25.35

Table S2. The stability of carbon-based Zn-air batteries has recently been reported.

Catalysts	Durability (h)	Reference
SnSb-NC	1106	This work
(Ni, Cu)-NG	110	7
Fe Co-WC/NC	200	9
Co_9S_8@Co/Mn-S, N-PC	210	10
Co/CeO_2-NCNA@CC	380	11
Fe/Ni@NPC-SiO_2/Zn	600	12
FeCo(α)-ACM	900	13

※ The actual stable time of the SnSb-NC-based Zn-air battery should be more than 1106 hours due to the three power outages encountered during the test.

References

[1] K. Ding, J. Hu, J. Luo, W. Jin, L. Zhao, L. Zheng, W. Yan, B. Weng, H. Hou and X. Ji, Confined N-$CoSe_2$ active sites boost bifunctional oxygen electrocatalysis for rechargeable Zn–air batteries, *Nano Energy*, 2022, **91**, 106675.

[2] Li, Y. Tang, T. Fu, Y. Xiang, Z. Xiong, Y. Si, C. Guo and Z. Jiang, S, N co-doped carbon nanotubes coupled with CoFe nanoparticles as an efficient bifunctional ORR/OER electrocatalyst for rechargeable Zn-air batteries, *Chem. Eng. J*., 2022, **429**, 132174.

[3] X. Liu, L. Wang, P. Yu, C. Tian, F. Sun, J. Ma, W. Li and H. Fu, A Stable Bifunctional Catalyst for Rechargeable Zinc-Air Batteries: Iron-Cobalt Nanoparticles Embedded in a Nitrogen-Doped 3D Carbon Matrix, *Angew. Chem. Int. Ed*., 2018, **57**, 16166-16170.

[4] Z. Y. Lu, B. Wang, Y. F. Hu, W. Liu, Y. Zhao, R. Yang, Z. Li, J. Luo, B. Chi, Z. Jiang, M. Li, S. Mu, S. Liao, J. Zhang and X. Sun, An Isolated Zinc-Cobalt Atomic Pair for Highly Active and Durable Oxygen Reduction, *Angew. Chem. Int. Ed*., 2019, **58**, 2622-2626.

[5] E. Negro, A. Delpeuch, K. Vezzu, G. Nawn, F. Bertasi, A. Ansaldo, V. Pellegrini, B. Dembinska, S. Zoladek, K. Miecznikowski, I.A. Rutkowska, M. Skunik-Nuckowska, P.J. Kulesza, F. Bonaccorso and V. Di Noto, Toward Pt-Free Anion-Exchange Membrane Fuel Cells: Fe-Sn Carbon Nitride-Graphene Core-Shell Electrocatalysts for the Oxygen Reduction Reaction, *Chem. Mater*., 2018, **30**, 2651-2659.

[6] Y. Ting and H. Chi, Designing Binary Ru-Sn Oxides with Optimized Performances for the Air Electrode of Rechargeable Zinc-Air Batteries, *ACS Appl. Mater. Inter.*, 2018, **10**, 10064-10075.

[7] Y. Cheng, H. Wu, J. Han, S. Zhong, S. Huang, S. Chu, S. Song, K. Reddy, X. Wang, S. Wu, X. Zhuang, I. Johnson, P. Liu and M. Chen, Atomic Ni and Cu co-anchored 3D nanoporous graphene as an efficient oxygen reduction electrocatalyst for zinc-air batteries, *Nanoscale*, 2021, **13**, 10862-10870.

[8] X. Zhu, D. Zhang, C. Chen, Q. Zhang, R. Liu, Z. Xia, L. Dai, R. Amal and X. Lu, Harnessing the interplay of Fe-Ni atom pairs embedded in nitrogen-doped carbon for bifunctional oxygen electrocatalysis, *Nano Energy*, 2020, **71**, 104597.

[9] L. Xu, S. Wu, D. Deng, C. Wang, J. Qian, G. Lu and H. Li, Fabricating highly active and stable tungsten carbide electrocatalyst for rechargeable zinc-air batteries: An approach of dual metal Co-adjusted the electronic structure, *J. Alloys Compd*., 2021, **868**, 159236.

[10] S. Rui, Z. Lu, F. Jiu, F. Ke and W. Ai, In situ produced Co_9S_8 nanoclusters/Co/Mn-S, N multi-doped 3D porous carbon derived from eriochrome black T as an effective bifunctional oxygen electrocatalyst for rechargeable Zn-air batteries, *J. Colloid Interf. Sci*., 2022, **608**, 2100-2110.

[11] S. Li, H. Zhang, L. Wu, H. Zhao, L. Li, C. Sun and B. An, Vacancy-engineered CeO_2/Co

heterostructure anchored on the nitrogen-doped porous carbon nanosheet arrays vertically grown on carbon cloth as an integrated cathode for the oxygen reduction reaction of rechargeable Zn-air battery, *J. Mater. Chem. A*, 2022, **10**, 9858-9868.

[12] B. R. Guo, J. N. Guo, W. L. Yang, X. Y. Tian, X. Wang, Z. H. Xiang and M. Wu, Highly dispersed iron/nickel dual-sites in hierarchical porous carbon materials as high-performance bifunctional oxygen electrocatalysts for Zn-air batteries, *Renewable Energ*, 2022, **201**, 117-124.

[13] C. Chen, D. Cheng, S. Liu, Z. Wang, M. Hu and K. Zhou, Engineering the multiscale structure of bifunctional oxygen electrocatalyst for highly efficient and ultrastable zinc-air battery, *Energy Storage Mater*., 2020, **24**, 402-411.